

**Cyclic Elastic-Plastic Strain Estimation
for Notched Shafts in Bending**

Steven M. Tipton
Assistant Professor
The University of Tulsa
Mechanical Engineering Department
600 South College Avenue
Tulsa, Oklahoma 74104
(918-631-3000, telefax 918-631-3556)

(Abstract for the Third International Conference on
Biaxial/Multiaxial Fatigue, April 3-6, Stuttgart, West Germany)

Conventional notch strain estimation routines utilize as input the elastic stress concentration factor and the cyclic stress strain curve. Several notch strain estimation techniques are examined and compared to an approach which also considers the distribution of multiaxial elastic stress and strain throughout the notch cross section. This is used to approximate the elastic-plastic stress and strain distribution after the onset of cyclic yielding. This information is useful not only for local strain-based crack initiation life predictions, but also for weight function approaches for the prediction of subsequent crack propagation.

The techniques under investigation are applied to sets of specimens with identical bending stress concentration factors, but whose geometries differ enough to affect the distribution of stress beneath the point of maximum stress. Stress concentration factors range from 1.5 to 2.0 on specimens with shoulder fillets and circumferential grooves. Elastic stresses and strains are analyzed using the finite element method for the filleted shafts and using Neuber's closed form solution for circumferential notches of hyperbolic profile. The conventional methods predict the same notch root strain for constant amplitude bending specimens with the same stress concentration factor regardless of the geometry. However, accounting for the subsurface stress distribution suggests that substantially differing notch root strains may develop. Predictions using all techniques are presented along with elastic stress and strain distributions for the geometries under investigation.

Introduction

The application of local strain-based fatigue damage parameters requires an assessment of the cyclic elastic-plastic strain (and/or stress) state in the immediate proximity of stress concentration factors. The use of elastic-plastic finite element methods to analyze stresses and strains in complex geometries is increasing. However, the fine grid refinement required to accurately model most engineering notches makes this approach less than practical from the standpoint of the everyday designer. Several techniques have been developed to predict notch elastic-plastic strains using only elastic stress information and cyclic material data [1-18]. The most popular has been the extension of Neuber's work [1] to cyclic loading [2]. Most approaches are applicable to uniaxial loading only and do not explicitly consider the existence of multiaxial stresses that develop at notches.

Conventional notch strain estimation routines are based on some form of the stress concentration factor, K_t . This basis for elastic stress information is limited by several considerations:

- (a) Such factors exist for only a finite number of geometries, and most engineering components do not lend themselves to characterization by a simple K_t .
- (b) K_t gives only the maximum elastic stress component and disregards the multiaxial stress state which develops even under uniaxial loading.
- (c) K_t provides no information about subsurface stresses.

This paper discusses an approach which utilizes the distribution of elastic multiaxial stress and strain throughout the cross section of a component containing a stress concentration. The approach assumes that the distribution of strain remains the same in the cross section even though the relationship between stress and strain is no longer elastic in the notch vicinity. For a given strain distribution, the cyclic stress-strain material data can then be used to compute the corresponding elastic-plastic stress distribution and applied external forces. The approach can predict very different notch root strains for components with identical stress concentration factors but whose geometries differ enough to affect their subsurface stress distribution. Conventional approaches, using only K_t to characterize elastic stresses, predict the same cyclic notch strain for the components just mentioned. The approach presented holds promise for design applications in light of the fact that elastic finite element analyses are becoming more practical for use in everyday design. The strain estimations permit the analyst to apply a wide range of local strain based fatigue damage parameters. Also, the elastic stress distribution required as input may be used with fracture mechanics weight function approaches to analyze fatigue crack propagation through the cross section [18].

Conventional Notch Strain Estimation Approaches

Many approaches have been developed to approximate notch elastic-plastic strain using elastic stress information [1-18]. The most popular approaches attempt to extend the results from Neuber's analytical solutions of shear stress and strain in prismatic notched bodies [1].

Most of these neglect the multiaxial stresses which develop at axially loaded notches, and therefore, tend to overpredict strain. This makes the approaches somewhat appealing from a design standpoint. Neuber's Rule is expressed as:

$$K_t^2 S_{nom} e_{nom} = \sigma_N \epsilon_N \quad (1)$$

$$\epsilon_N = \frac{\sigma_N}{E} + \left[\frac{\sigma_N}{K'} \right]^{1/n'} \quad e_{nom} = \frac{S_{nom}}{E} + \left[\frac{S_{nom}}{K'} \right]^{1/n'} \quad (2)$$

where

S_{nom} = nominal stress at notch location

e_{nom} = nominal strain at notch location

σ_N = notch stress

ϵ_N = notch elastic - plastic strain from Neuber

E = elastic modulus

K' = cyclic strain hardening coefficient

n' = cyclic strain hardening exponent

The elastic-plastic relation for nominal stress and strain is used to account for higher loading amplitudes. The assumption is made that plane sections remain plane so that the bending strain gradient is linear. The resulting stress distribution, times the distance from the neutral axis, may be integrated over the cross section to compute the applied external moment. For further details, see Refs. [17-19].

Glinka [15,16] developed a notch strain estimation routine based on the concept of equivalent strain energy density. The approach is based on the assumption that the distribution of elastic strain energy density in the notch tip vicinity remains the same after localized cyclic yielding occurs. The approach has been successfully applied to notched flat plates under a variety of loading conditions. A version of Glinka's approach is presented below for plane stress situations.

$$\frac{\sigma_p^2}{2E} + \frac{\sigma_p}{n'+1} \left[\frac{\sigma_p}{K'} \right]^{1/n'} = \frac{S_{nom}^2}{2E} + \frac{S_{nom}}{n'+1} \left[\frac{S_{nom}}{K'} \right]^{1/n'} K_t^2 \quad (3)$$

$$\epsilon_p = \frac{\sigma_p}{E} + \left[\frac{\sigma_p}{K'} \right]^{1/n'} \quad (4)$$

where

σ_p = Glinka notch stress estimation

ϵ_p = Glinka notch strain estimation

The nominal stress and strain are related as in Eqn. 2 and the applied external load must be found accordingly. The Glinka and Neuber approaches are applied as outlined below:

- (a) Choose e_{nom} , the nominal surface strain.
- (b) The distribution of nominal strain is considered linear, therefore the nominal stress distribution is found from Eqn. 2.

- (c) The product of the nominal stress at a given location, times the distance from the neutral bending axis is integrated throughout the cross section to compute the corresponding external applied bending moment.
- (d) With M computed for a given S_{nom} and ϵ_{nom} , the notch stress and strain may be estimated using Eqns. 1 and 2 for the Neuber analysis and Eqns. 3 and 4 for the Glinka approach.

Strain Distribution Technique

This approach is similar to that described in Refs. [17&18]. The distribution of multiaxial elastic strains in bending is assumed to remain the same even after the onset of plasticity at the notch. Given the axial strain distribution, the stress distribution may be computed with the cyclic stress strain curve and used to determine the corresponding applied loading. To apply the approach, the following steps are taken.

- (a) The distribution of elastic, axial strain is obtained through the cross section containing the notch. This will usually be determined from an elastic finite element analysis. For the circumferentially notched shafts examined here, a piecewise linear approximation of the strain distribution along a radial line below the maximum strain location is sufficient [17,18].
- (b) The stress distribution is computed through the cross section using the uniaxial cyclic stress-strain relation for the material. This neglects the multiaxiality of through-section stresses as demonstrated in Fig. 2 and 3.
- (c) The product of the stress times the distance from the neutral bending axis is integrated over the entire cross section to obtain the corresponding applied external loading.

For circular cross sections, this integration need only be made along a radial line beneath the point of maximum stress [17,18]. For general cross sections a first order numerical scheme is adequate if a sufficient number of integration points are defined in the steep section of the distribution near the notch root. The BASIC program used to generate the moment versus notch strain estimations for round shafts using a piecewise linear approximation of the strain distribution is presented in the Appendix.

Specimen Geometries and Material Properties

The three approaches described above are applied to sets of specimens with identical elastic bending stress concentration factors, but very different elastic stress distributions. Shoulder filleted shafts are modeled using axisymmetric finite elements, and a typical mesh cross section is shown in Fig. 1. The meshes were specifically designed with a fine grid at the notch to capture the sharp notch stress gradients. Stress concentration factors predicted from the finite element analyses were within 2% of values from Peterson's handbook [20]. Neuber [21] developed a closed form solution to the elastic stresses in a circular shaft with a circumferential groove of hyperbolic profile. Figure 1 presents both geometries and the stress concentration factors examined in this study. Figures 2(a) and 3(a) present multiaxial elastic stress distributions for stress concentration factors of 2.04 and 1.53, respectively, normalized by the nominal elastic stress at the notch root. The elastic strain distribution for each geometry is also

shown in Figs. 2(b) and 3(b), normalized by the nominal elastic strain at the notch root. At any point along the radius, the normalized elastic axial strain is computed from the elastic stress components by:

$$\frac{\epsilon_z}{e_{nom}} = \frac{\sigma_z}{S_e} - \mu \left[\frac{\sigma_\theta}{S_e} + \frac{\sigma_r}{S_e} \right] \quad (5)$$

where

σ_z, σ_θ and σ_r = axial, circumferential and radial elastic stress

ϵ_z = axial elastic strain

e_{nom} = nominal elastic strain

S_e = nominal elastic stress = e_{nom}/E

μ = Poisson's ratio = 0.3

Notice from Figs. 2 and 3 that the constraint on transverse stresses at the notch root results in normalized axial strain distributions which are considerably lower than corresponding axial stress distributions.

A net section diameter of 40 mm was chosen for all specimens and the corresponding curves for bending moment versus notch strain computed using the three notch strain estimation procedures described above. The material properties for normalized 1045 steel of $E=202375$ MPa, $K'=1286$ MPa and $n'=0.2124$ are used in all cases and Poisson's ratio was chosen to be 0.3. The strain estimations are presented in Figs. 4-6 and are discussed below. It should be noted that the finite element models were loaded in cantilevered bending while Neuber's grooved shaft solutions are for pure bending. The difference is assumed negligible for this analysis.

Strain Estimations

From the curves in Figs. 4-6, the following observations can be made. The strains estimated for the filleted shaft are considerably lower than those for the grooved shafts, using the strain distribution approach. (For a strain amplitude of 0.007 in the grooved shaft, which corresponds to a fatigue life of a few thousand cycles for normalized 1045, the fillet strains are predicted to be about 40% lower.) The other routines predict the same notch strains for either geometry. Note that for the relatively mild stress concentration factors of 1.68 and 1.53, the Neuber and Glinka approaches correlate well with the strain distribution approach for the filleted shafts. The predictions for the "higher" stress concentration factor of 2.0 show decreased correlation. For the sake of comparison, the three methods described in this paper are applied to the shaft shown in Fig. 7, using elastic stress data from Ref. [22]. The predictions are shown in Fig. 8, along with stabilized bending strain amplitude data, measured with strain gage rosettes [17,18]. Figure 8 shows that the strain distribution approach is comparable to the other two approaches in making adequate notch strain estimations. The approaches all tend to overpredict strains, but this could be explained by physical considerations involving the use strain gages in sharp notches. This is discussed in the next section.

Discussion

A point must be made concerning the assumptions used to implement the Neuber and Glinka approaches. The Neuber approach would predict different notch root strains for the filleted shaft and grooved shaft if the fatigue notch factor, K_f , were used instead of K_t [2]. However, note from Fig. 1 that the notch root radii for the hyperbolic grooves are considerably larger than the corresponding fillet radii. Using empirical relations [23] would result in a lower K_f for the grooved shaft and, therefore in lower strain estimates. It should also be noted here that Glinka [16] presents a modification to Eqns. (3) and (4) which account for the plastic redistribution of notch root stress and strain near the notch tip. This would change the predictions slightly for the mild notches examined in this paper but would not produce different estimations between filleted and grooved specimens. Hoffman and Seeger [14] developed a modularized approach which requires assumption or input data regarding the notch constraint on transverse surface strains during cyclic plastic loading. It is shown that for grooved shafts in tension, the ratio of axial to circumferential surface strains may be assumed constant as elastic strains become elastic-plastic. This assumption is used with an appropriate empirical relation between notch and nominal stress (such as Neuber's rule) and appropriate plasticity relations to relate notch strains to applied loading. Since the circumferential elastic stress at the notch is similar for the filleted and grooved specimens (Figs. 2 and 3), the approach would not predict significantly differing notch strains between the two specimens.

The use of the elastic strain distribution for the approach proposed in this paper has advantages from several standpoints. The majority of engineering components do not lend themselves to simple characterization by a single stress concentration factor. For instance, consider the lifting hook shown in Fig. 9(a). No reliable stress concentration factors can be found for this geometry, particularly considering the noncircular cross section. To investigate elastic stresses in this situation, a finite element model is necessary, such as that shown in Fig. 9(b). From the finite element solution for stresses in the critical cross sections (two are considered critical), elastic strain distributions can be directly used with the method in this paper to compute the elastic-plastic cyclic strains. This is important in light of the fact that finite element analyses are becoming more practical from the standpoint of everyday design. For example, the finite element model shown in Fig. 9(b) is being implemented using a personal-computer based finite element routine [24].

At the current time, no experimental data is available for direct comparison to the predictions made in this paper (other than those presented in Fig. 8). Specimens are currently being designed with a testing program to address the other questions raised in this study. The current plans are to limit the experimental investigation to the relatively mild stress concentration factor range of 1.5 to 2.0. This is due to the difficulty in experimentally measuring strains at notch root radii much smaller than those presented in Fig. 1. A small notch radius on a cylindrical specimen makes it difficult to physically mount a strain gage rosette. Also, the placement of the gage within the notch is critical due to the rapidly changing strain along the surface of the notch root. Figure 10 shows the notch surface stress distribution for a specimen

whose stress concentration factor is 1.5. This figure reveals that a gage must be placed slightly up the notch from the tangent point of the fillet radius in order to measure the peak strain. A gage mounted to either side of the peak could measure a substantially lower strain. The figure also points out the importance of gage size. The physical size of a strain gage, which can only measure the average strain of the material it covers, could read a lower strain than the peak value, even if mounted directly on the peak. This may partially explain the overprediction of the strain data in Fig. 8.

The simplified version of the strain distribution technique presented in this paper is only demonstrated for fully-reversed, constant amplitude bending loading. For this situation the approach uses an assumption similar to the "plane sections remaining plane" assumption used to compute the nominal stress in a smooth bar in bending [19]. The technique assumes that the geometric shape of the strain distribution will not change significantly due to localized notch yielding. This converts the notch strain estimation problem into a strain-controlled plasticity problem. (Appropriate constitutive relations are used to compute stress distribution from the assumed strain distribution and then integrated to arrive at the applied external loading associated with the notch surface strain.) The approach presented in this paper uses the uniaxial cyclic stress-strain curve to estimate the stress distribution from the assumed strain distribution. The multiaxiality of the strain distribution is not considered in the current version of this approach. Several modifications to the approach are being investigated which do account, in a more general sense, for notch multiaxial stress and strain distribution. The technique resembles the modular approach of Hoffman and Seeger [16], except that the multiaxial elastic-plastic strain distribution must be approximated from the elastic strain distribution, and an appropriate plasticity relation is applied throughout the cross section. This is integrated to ultimately find the corresponding external loading on the component. The use of an appropriate hardening relation can account for cyclic hardening or softening. This can be of major consequence since the cyclic hardening or softening rate for a material is dependent on the cyclic strain amplitude which varies throughout the cross section [see Ref. 19]. The approach can be worked into a subroutine which interfaces directly with elastic finite element output to predict elastic-plastic strain and stress in a section of interest.

Conclusions

A technique is presented which predicts bending strains in circumferentially notched components. The technique assumes that the elastic distribution of multiaxial strain remains unchanged with the onset of localized notch plasticity. The approach predicts very different notch root strains for specimens with identical elastic stress concentration factors but differing subsurface stress distributions. Conventional notch strain estimation routines are shown to predict the same notch root strain for a given K_t regardless of the stress distribution. The strain distribution approach is shown to be applicable to general engineering components whose elastic stresses are found using finite element analysis. Tests are underway to substantiate the approach and to direct the development of a more sophisticated version.

Acknowledgements

The author would like to express appreciation to the National Science Foundation for supporting this research (NSF EPSCoR Grant Number RII 8610676).

References

1. Neuber, H., "Theory of Stress Concentration for Shear Strained Prismatical Bodies with Arbitrary Nonlinear Stress-Strain Law," Journal of Applied Mechanics, Dec. 1961, pp. 544-550.
2. Topper, T. H., Wetzel, R. M., and Morrow, JoDean, "Neuber's rule Applied to Fatigue of Notched Specimens," Naval Air Engineering Center, Aeronautical Structures Laboratory, Report No. 1114, June, 1976, also in Journal of Materials, JMLSA, Vol. 4, No. 1, March 1969, pp. 200-209.
3. Crews, J. H. Jr., and Hardrath, H. F., "A Study of Cyclic Plastic Stresses at a Notch Root," Experimental Mechanics, Vol. 6, June 1966, pp. 313-320.
4. Manson, S. S., and Hirschberg, M. H., "Crack Initiation and Propagation in Notched Fatigue Specimens," National Aeronautics and Space Administration, Technical Memorandum X-52126, 1965.
5. Topper, T. H., Wetzel, R. M., and Morrow, JoDean, "Neuber's Rule Applied to Fatigue of Notched Specimens," Naval Air engineering Center, Aeronautical Structures Laboratory, Report No. 1114, June, 1976, also in Journal of Materials, JMLSA, Vol. 4, No. 1, March 1969, pp. 200-209.
6. Wetzel, R. M., "Smooth Specimen Simulation of the Fatigue Behavior of Notches," Journal of Materials, JMLSA, Vol. 3, No. 3, September 1969, pp. 646-657.
7. Impellizzeri, L. F., "Cumulative Damage Analysis in Structural Fatigue," Effects of Environment and Complex Load History on Fatigue Life, ASTM STP 462, American Society for Testing and Materials, 1970, pp. 40-68.
8. Paprino, R., "Plastic Stress-Strain History at Notch Roots in Tensile Strips Under Monotonic Loading," Experimental Mechanics, October 1971, pp. 446-452.
9. Gonyea, D. C., "Method for Low-Cycle Fatigue Design Including Biaxial Stress and Notch Effects," Fatigue at Elevated Temperatures, ASTM STP 520, American Society for Testing and Materials, 1973, pp. 678-687.
10. Kotani, S., Koibuchi, K., and Kasai, K., "The Effect of Notches on Cyclic Stress-Strain Behavior and Fatigue Crack Initiation," Proc. Second Intl. Conf. on Mechanical Behavior of Materials, Boston, Mass., August 1976.
11. Nelson, D. V., Cumulative Fatigue Damage in Metals, Ph.D. Dissertation, Mechanical Engineering Department, Stanford University, Stanford, California, March 1978, pp.

12. Dowling, N. E., Brose, W. R., and Wilson, W. K., "Notched Member Fatigue Life Predictions by the Local Strain Approach," Fatigue under Complex Loading, Vol. 6 of Advances in Engineering, R. M. Wetzell, ed., SAE, Warrendale, PA, 1977.
13. Hoffmann, M., and Seeger, T., "Ermittlung und Beschreibung mehrachsiger Kerbbeanspruchungen im nichtlinearen Bereich Teil 3," Publication FB-2/1983, Fachgebiet Werkstoffmechanik der Technischen Hochschule Darmstadt, Federal Republic of Germany, 1983.
14. Hoffmann, M., and Seeger, T., "A Generalized Method for Estimating Multiaxial Elastic-Plastic Notch Stresses and Strains, Parts 1 and 2" Journal of Engineering Materials and Technology, Transactions of the ASME, Vol. 107, pp. 250-258, 1985.
15. Molski, K., and Glinka, G., "A Method of Elastic-Plastic Stress and Strain Calculation at a Notch Root," Mat. Sci. Eng., Vol. 50, pp. 93-100, 1981.
16. Glinka, G., "Calculation of Inelastic Notch-Tip Strain-Stress Histories Under Cyclic Loading," Eng. Frac. Mech., Vol. 22, No. 5, pp. 839-845, 1985.
17. Tipton, S. M., Fatigue Behavior under Multiaxial Loading in the Presence of a Notch: Methodologies for the Prediction of Life to Crack Initiation and Life Spent in Crack Propagation, Ph.D. dissertation, Stanford University, Stanford, California, Jan. 1985.
18. Tipton, S. M., and Nelson, D. V., "Methods for Estimating Stabilized Cyclic Notch Strains in the SAE Specimen," Society of Automotive Engineers, AE, Multiaxial Fatigue, 1989.
19. Dowling, N.E., "Stress-Strain Analysis of Cyclic Plastic Bending and Torsion," Journal of Engineering Materials and Technology, Transactions of the ASME, Vol 100, pp. 157-163, 1978.
20. Peterson, R.E., Stress Concentration Factors, John Wiley and Sons, New York, 1974.
21. Neuber, H., Kerbspannunglehre, Springer, Berlin (1937), Translation, Theory of Notch Stresses, J.W. Edwards Co., Ann Arbor, MI, pp. 116-136, 1946.
22. Chang, S.S. and Johnson, K.V., "Predicting Fatigue Life in Biaxial Stress Fields," Bucyrus-Erie Company, paper presented to the Society of Automotive Engineers Fatigue Design and Evaluation Committee, April 30, 1987, Cincinnati, OH.
23. Sines, G. and Waisman, J.L., Metal Fatigue, McGraw-Hill, New York, p. 296, 1959.
24. Verbal Communication with L. Crandall, Chief Engineer, Crosby-McKissick Inc., Tulsa, OK, Jan., 1989. ALGOR Finite Element Code, Pittsburgh, PA.

Appendix

```
10 REM *****
20 REM * THIS PROGRAM COMPUTES THE CYCLIC NOTCH STRAIN ON A CYLINDRICAL*
30 REM * SPECIMEN FOR CONSTANT AMPLITUDE, FULLY REVERSED LOADING. *
40 REM * PREDICTIONS ARE SENT TO A FILE NAMED: "CNS.DAT". NPTS DATA *
60 REM * POINTS ARE GENERATED OVER AN ENOM RANGE FROM 0 TO EMAX *
60 REM *****
70 REM
80 OPEN "O",#1,"CNS.DAT"
90 DIM Y(101),ES(101),G(101),YNORM(101),ENORM(101)
100 N=100 :REM THIS IS THE NUMBER OF STEPS FOR SIMPSON'S RULE INTEGRATION
110 NPTS=50
120 EMAX=.005
130 NN=N+1
140 E=2023751 :REM ELASTIC MODULUS
150 KP=1286 :REM CYCLIC STRAIN HARDENING COEFFICIENT
160 NP=.2124 :REM CYCLIC STRAIN HARDENING EXPONENT
170 R=.02 :REM SPECIMEN RADIUS AT NOTCH ROOT
180 H=R/N :REM SIMPSON'S RULE STEPSIZE
190 ENOM=0! :REM INITIALIZATION
200 SIG=5! :REM INITIALIZATION
210 NSEG=7 :REM NUMBER OF LINEAR STRAIN SEGMENTS
220 REM NEXT NSEG LINES ARE NORMALIZED RADIAL POSITIONS
230 YSEG(1)=.5
240 YSEG(2)=.6
250 YSEG(3)=.7
260 YSEG(4)=.8
270 YSEG(5)=.9
280 YSEG(6)=.97
290 YSEG(7)=1!
300 REM NEXT NSEG LINES ARE NORMALIZED NORMAL BENDING STRAINS
310 ESEG(1)=.350125
320 ESEG(2)=.42031
330 ESEG(3)=.497555
340 ESEG(4)=.61336
350 ESEG(5)=.8116
360 ESEG(6)=1.0775
370 ESEG(7)=1.38
380 REM NEXT 13 LINES COMPUTES NORMALIZED STRAIN DISTRIBUTION
390 REM FOR COMPUTING SIMPSON'S RULE INTEGRAND
400 Y1=0
410 E1=0
420 NTEST=1
430 FOR K=1 TO NN
440 YNORM(K)=(K*H/R)-H/R
450 IF YNORM(K) > YSEG(NTEST) THEN 480
460 ENORM(K)=E1+(YNORM(K)-Y1)*(ESEG(NTEST)-E1)/(YSEG(NTEST)-Y1)
470 GOTO 520
480 Y1=YSEG(NTEST)
490 E1=ESEG(NTEST)
500 NTEST=NTEST+1
510 GOTO 450
520 NEXT K
530 PRINT " MOMENT NOTCH STRN NOM STRN STRESS"
540 REM MAIN PROGRAM
550 REM
560 FOR I=1 TO NPTS :REM "I" LOOP STEPS THROUGH ENOM INCREMENTS
570 ENOM=ENOM+EMAX/NPTS
580 REM
590 EP=ENORM(101)*ENOM :REM EP = PLASTIC SURFACE STRAIN
600 FOR J=1 TO NN :REM THIS "J" LOOP COMPUTES STRAIN DISTRIBUTION
610 Y(J)=YNORM(J)*R
620 ES(J)=ENOM*ENORM(J)
630 NEXT J
640 FOR J=2 TO NN :REM THIS "J" LOOP COMPUTES STRESS DISTRIBUTION
650 ESS=ES(J) :REM AND SIMPSON'S RULE INTEGRAND, G(J)
660 FSIG=SIG/E+(SIG/KP)^(1/NP)-ESS
670 FPSIG=(1/E)+((1/KP)^(1/NP))*(1/NP)*SIG^(1/NP-1)
680 SIGP=SIG-FSIG/FPSIG
690 IF ABS(SIGP-SIG) <= .01 THEN 720
700 SIG=SIGP
710 GOTO 660
720 SIG=SIGP :REM SIG=ELASTIC-PLASTIC STRESS -(NEWTON-RAPHSON)
730 G(J)=SIG*Y(J)*SQR(R*R-Y(J)*Y(J))
740 NEXT J
750 REM
760 REM SIMPSON'S RULE INTEGRATION
770 REM
780 M=4*H*(G(101)+4*G(100))/3
790 NM=N/2-1
800 FOR J=1 TO NM
810 NODD=2*J
820 NEVEN=2*J+1
830 M=M+4*H*(4*G(NODD)+2*G(NEVEN))/3
840 NEXT J
850 M=M*1000000! :REM APPLIED EXTERNAL BENDING MOMENT
860 PRINT USING "#####.## 0.##### 0.##### 0####.##";M,EP,ENOM,SIG
870 PRINT#1,USING "#####.## 0.##### 0.##### 0####.##";M;EP;ENOM;SIG
880 NEXT I
890 CLOSE #1
900 END
```

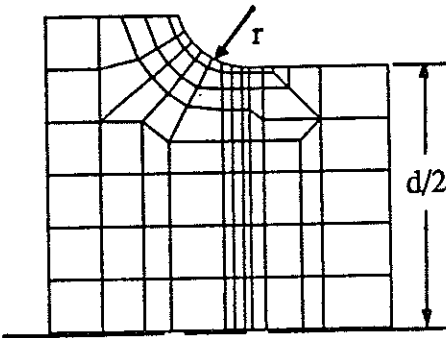
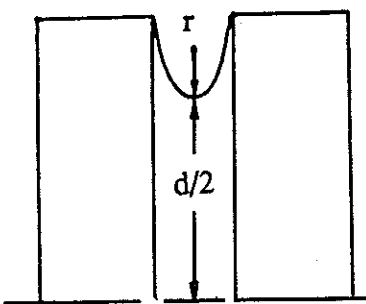
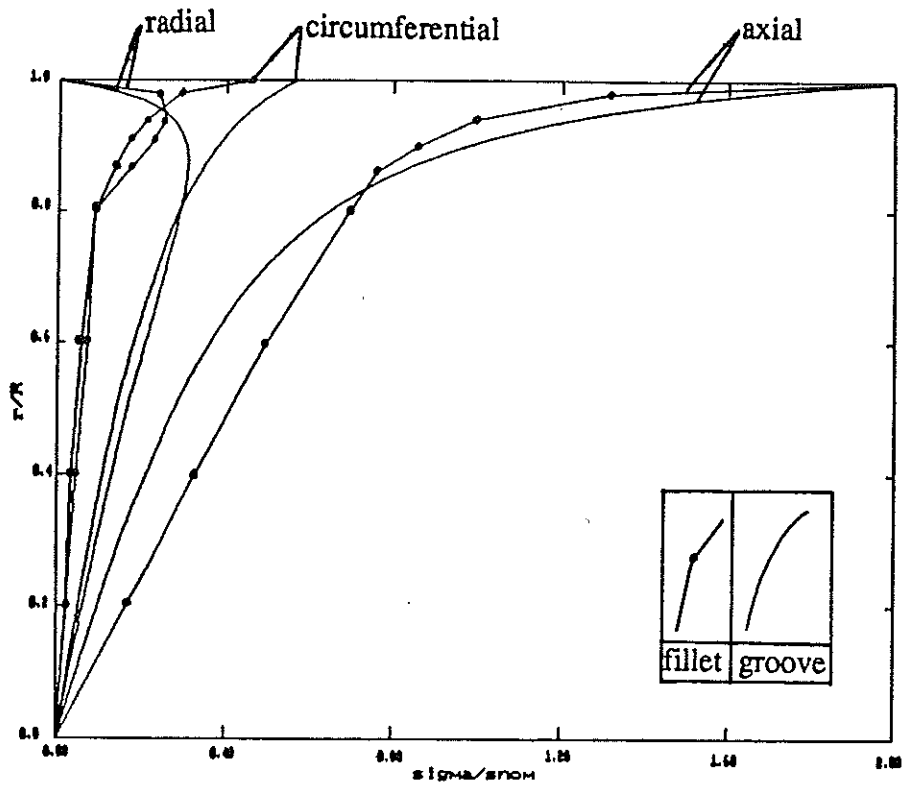
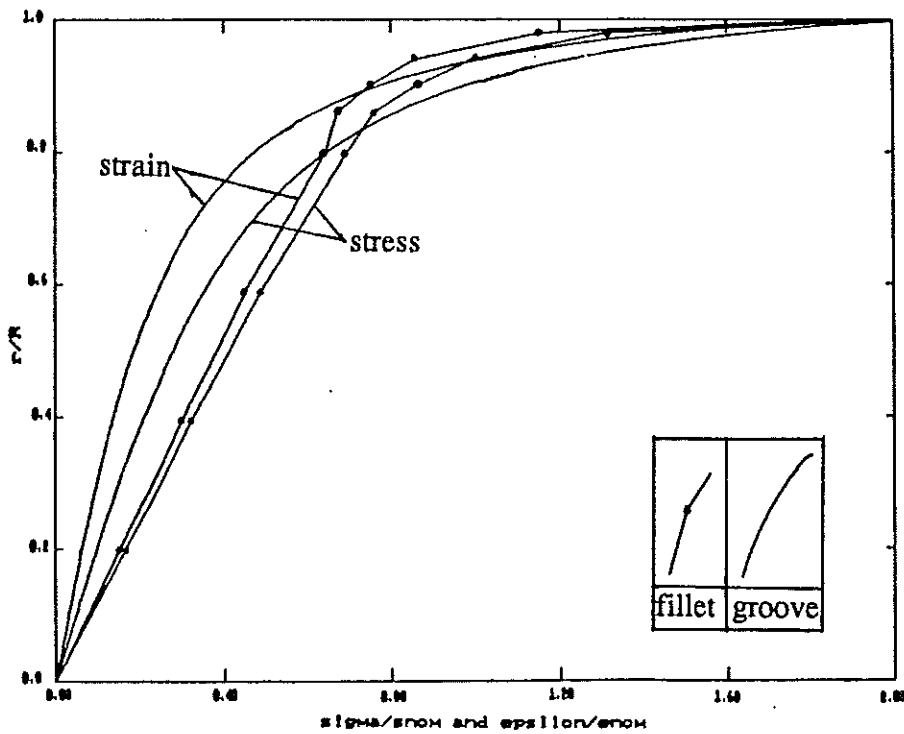
K_t	Finite Element Mesh, Fillet 	Neuber [21] Grooved Shaft 
2.04	$r/d = 0.047$	$r/d = 0.189$
1.68	$r/d = 0.096$	$r/d = 0.328$
1.53	$r/d = 0.28$	$r/d = 0.446$

Figure 1: Geometry of filleted shafts and grooved shafts.

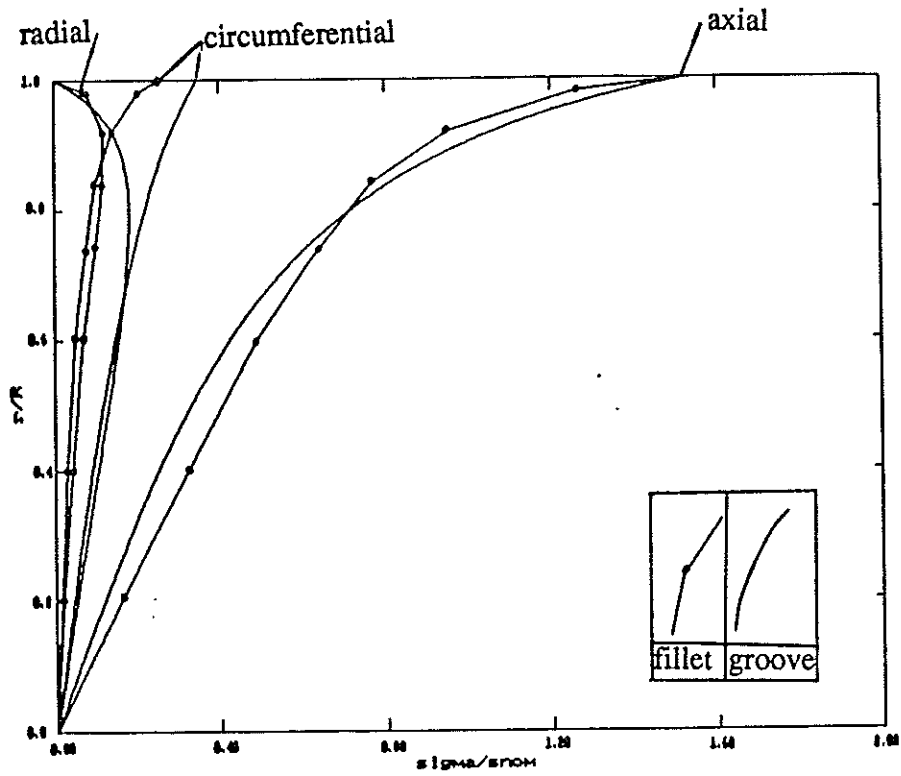


(a)

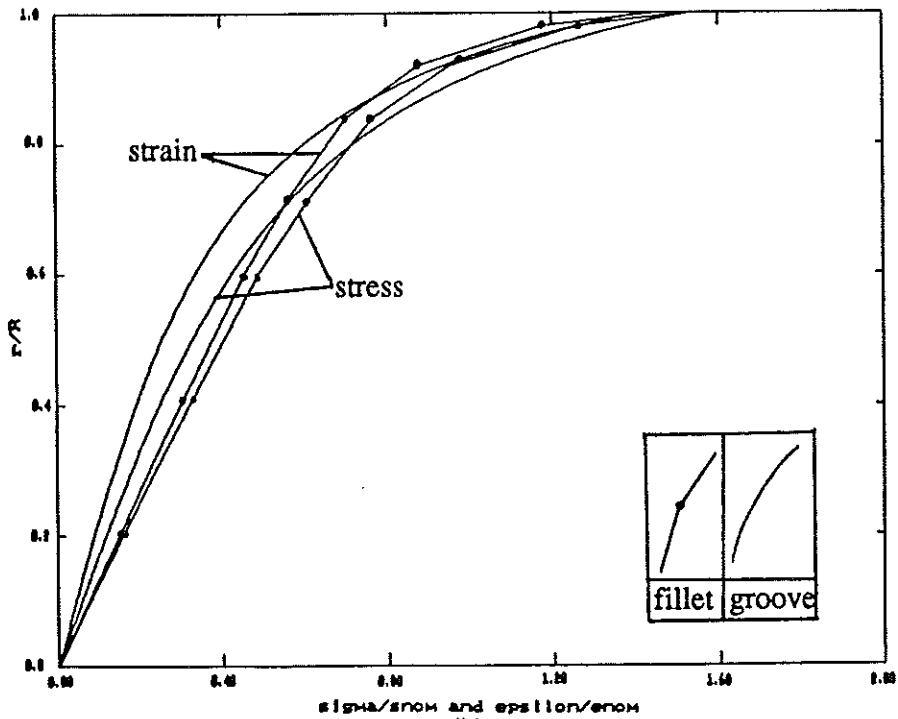


(b)

Figure 2: (a) Normalized distribution of multi-axial stress components in filleted and grooved shaft due to bending ($K_t=2.04$). (b) Normalized axial stress and strain distribution.



(a)



(b)

Figure 3: (a) Normalized distribution of multiaxial stress components in filleted and grooved shaft due to bending ($K_t=1.53$). (b) Normalized axial stress and strain distribution.

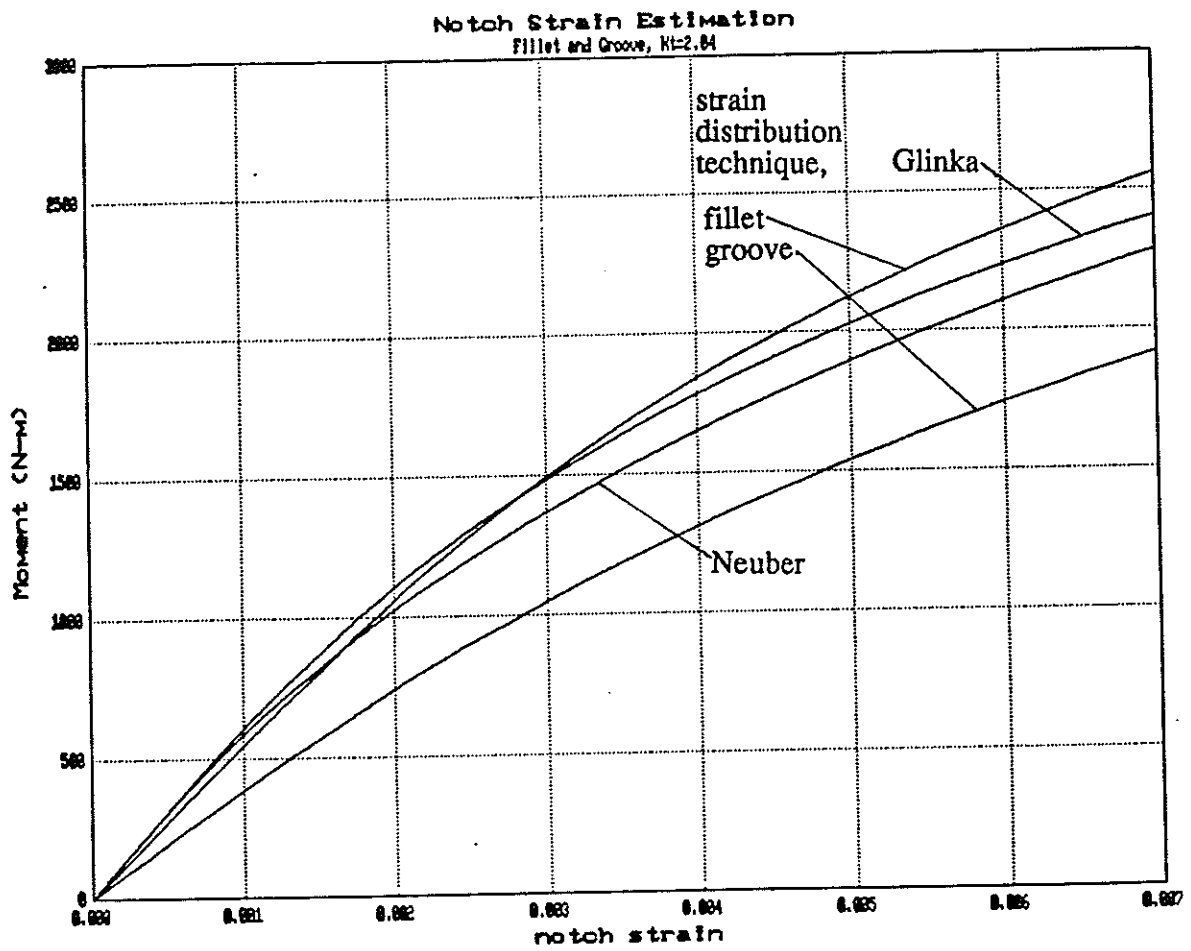


Figure 4: Elastic-plastic notch strain estimates from Neuber, Glinka and strain distribution approaches for filleted and grooved specimens, $K_t=2.04$.

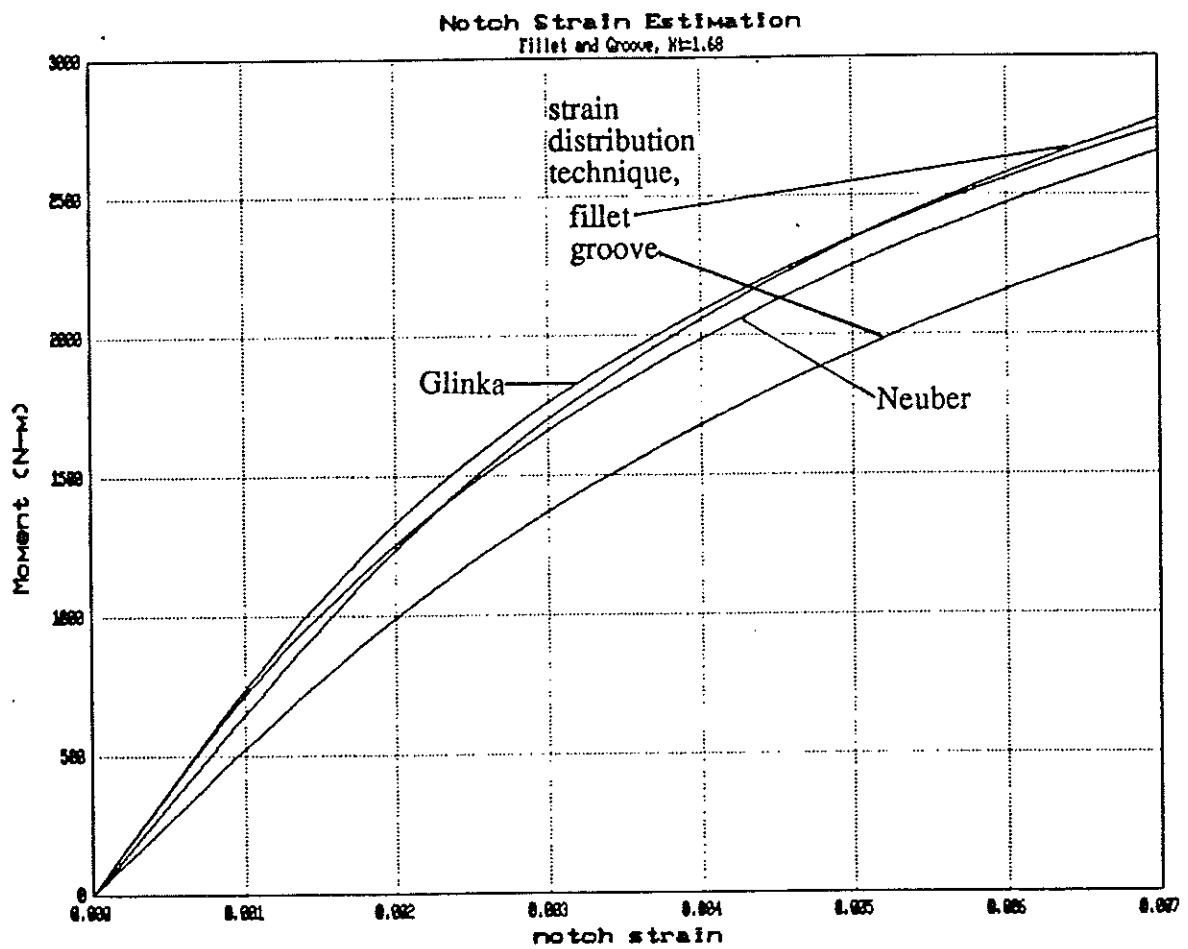


Figure 5: Elastic-plastic notch strain estimates from Neuber, Glinka and strain distribution approaches for filleted and grooved specimens, $K_t=1.68$.

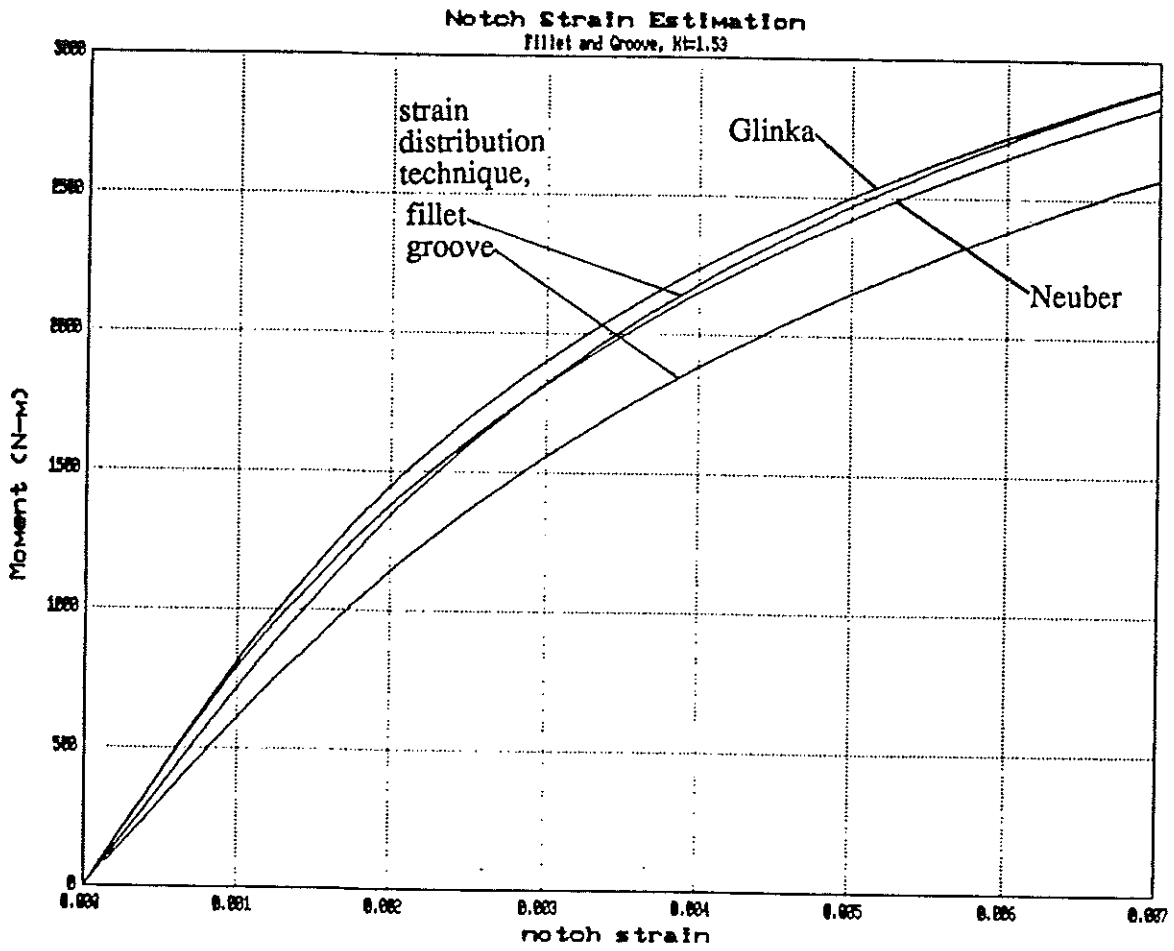


Figure 6: Elastic-plastic notch strain estimates from Neuber, Glinka and strain distribution approaches for filleted and grooved specimens, $K_t=1.53$.

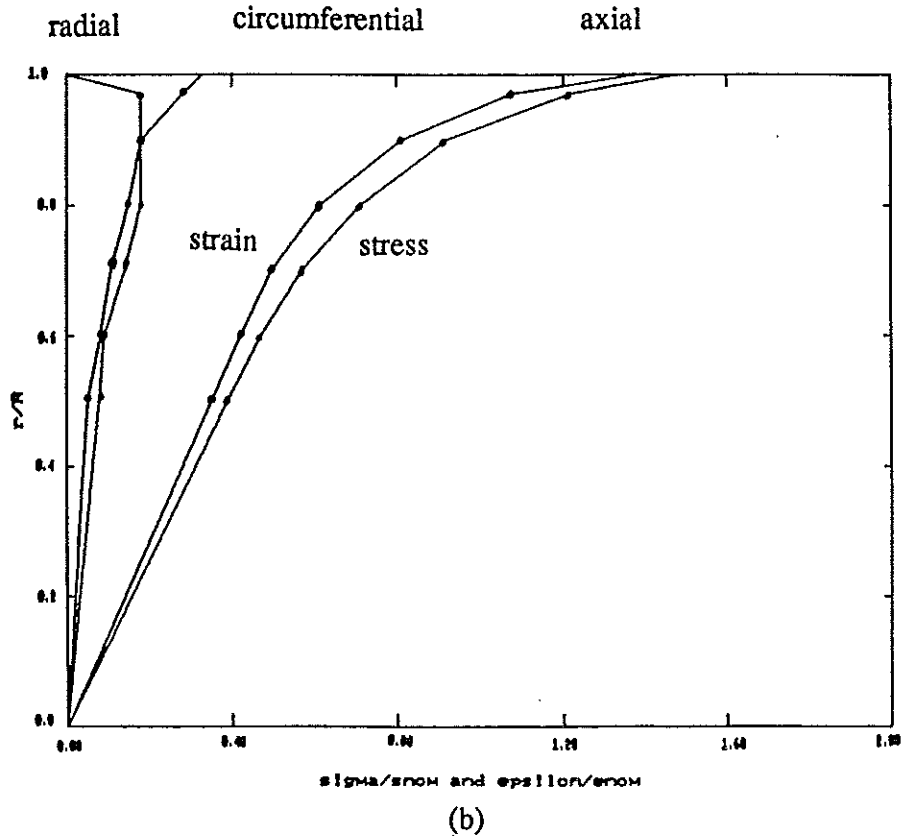
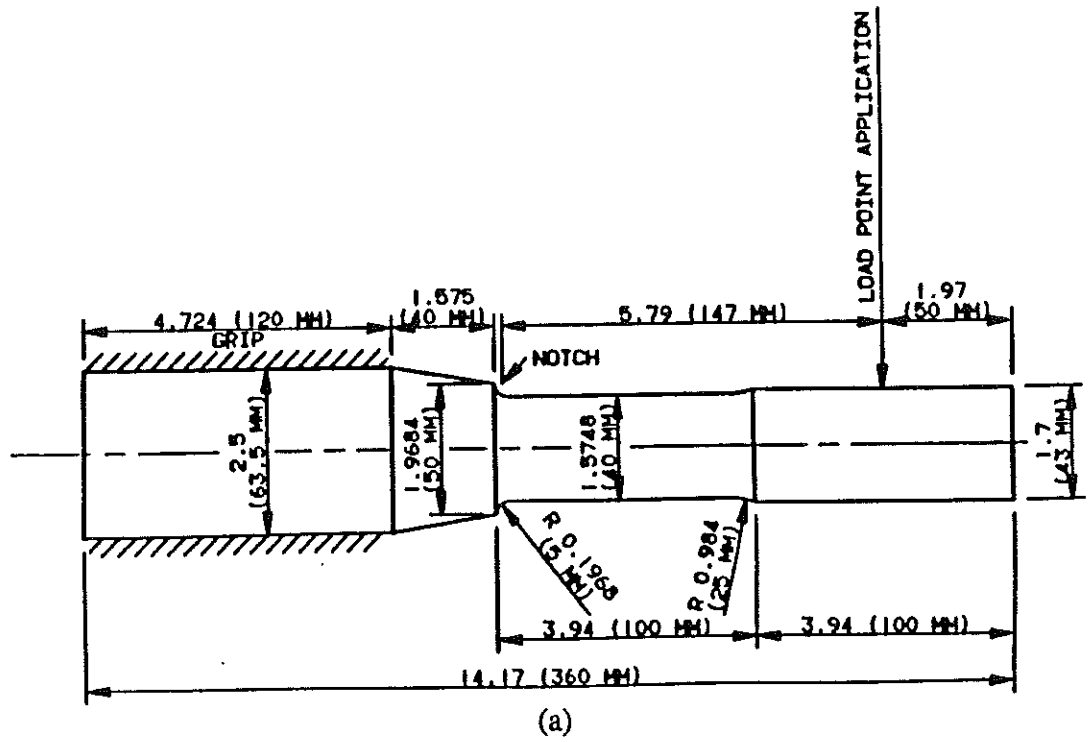


Figure 7: (a) Society of Automotive Engineers Fatigue Design and Evaluation Committee filleted shaft specimen. (b) Normalized distribution of multiaxial elastic stress in SAE specimen [22].

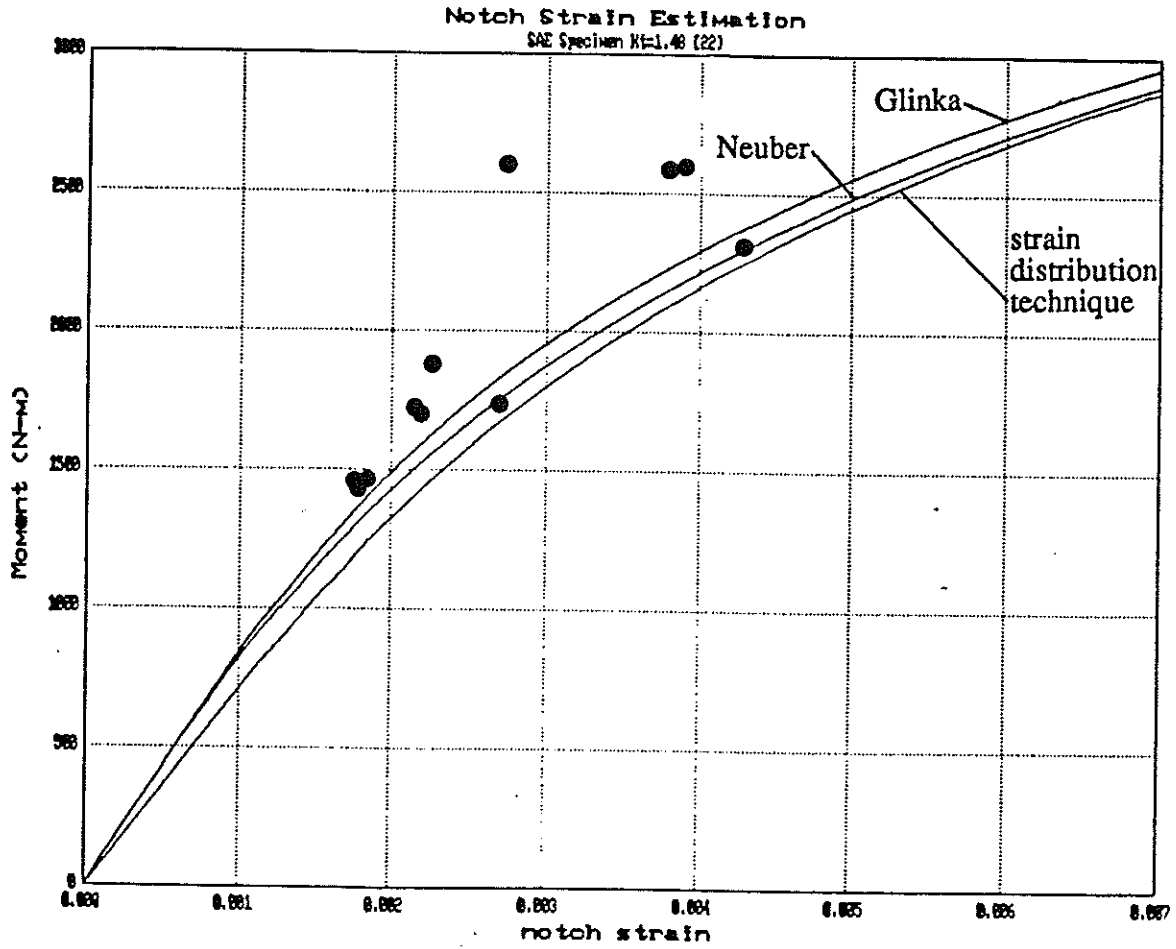


Figure 8: Elastic-plastic notch strain estimates from Neuber, Glinka and strain distribution approaches for filleted SAE specimen compared to strain gage data.

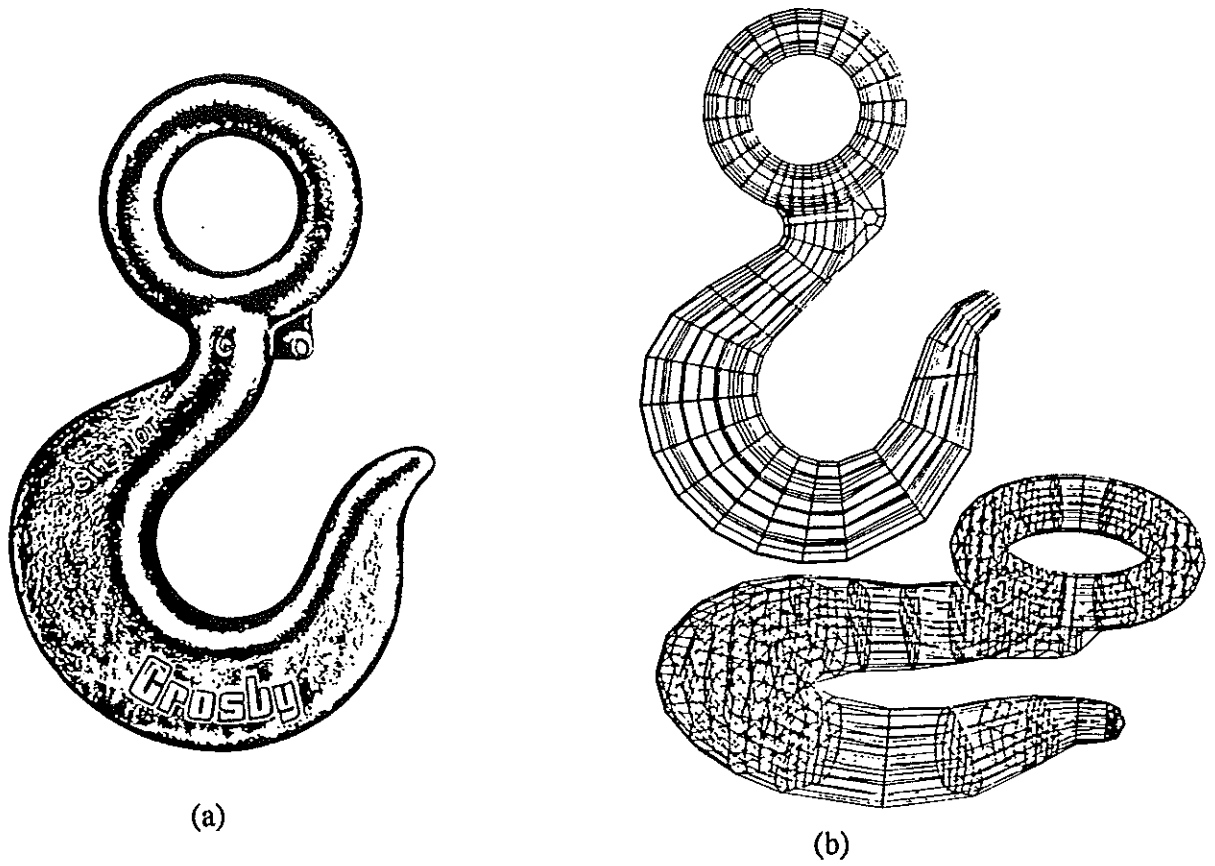


Figure 9: (a) Lifting hook from Crosby McKissick, Inc., Tulsa, Oklahoma. (b) Three dimensional finite element model of lifting hook for use in ALGOR personal computer finite element algorithm.

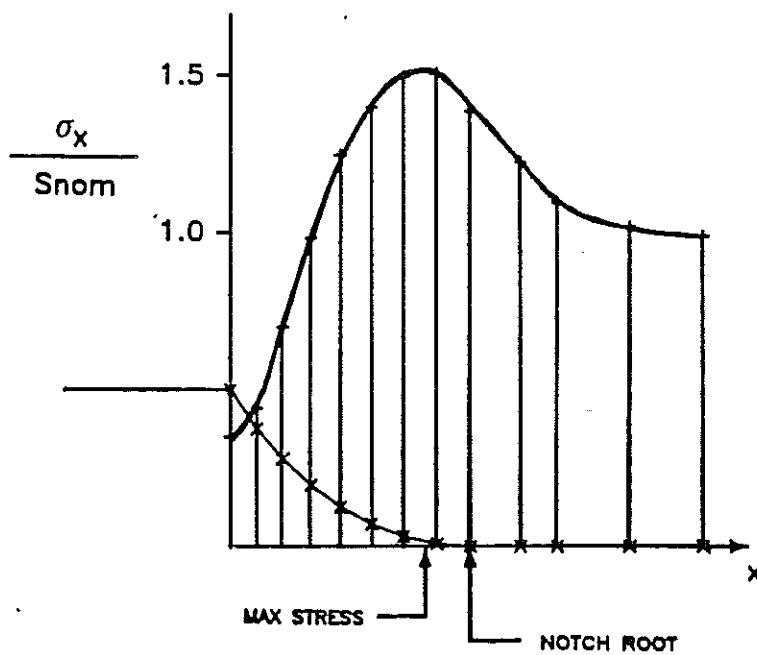


Figure 10: Distribution of elastic stress along the surface of the fillet ($K_t=1.53$).